Neuron, Vol. 32, 301–313, October 25, 2001, Copyright ©2001 by Cell Press

Multivesicular Release at Climbing Fiber-Purkinje Cell Synapses

Jacques I. Wadiche and Craig E. Jahr[1]
Vollum Institute
Oregon Health Sciences University L474
3181 S. W. Sam Jackson Park Road
Portland, Oregon 97201

Summary

Synapses driven by action potentials are thought to release transmitter in an all-or-none fashion; either one synaptic vesicle undergoes exocytosis, or there is no release. We have estimated the glutamate concentration transient at climbing fiber synapses on Purkinje cells by measuring the inhibition of excitatory postsynaptic currents (EPSCs) produced by a low-affinity competitive antagonist of AMPA receptors, γ-DGG. The results, together with simulations using a kinetic model of the AMPA receptor, suggest that the peak glutamate concentration at this synapse is dependent on release probability but is not affected by pooling of transmitter released from neighboring synapses. We propose that the mechanism responsible for the elevated glutamate concentration at this synapse is the simultaneous release of multiple vesicles per site.

Introduction

At specialized presynaptic release sites, defined ultrastructurally by presynaptic and postsynaptic membrane specializations and a cluster of vesicles in the presynaptic structure, neurotransmitter is released into the synaptic cleft by vesicular exocytosis. A tenet of the release process is that a maximum of one vesicle per synaptic connection is released in a probabilistic manner with each action potential (Redman, 1990; Korn et al., 1994), despite an excess of vesicles apparently docked at the presynaptic membrane (e.g., Sorra and Harris, 1993; Schikorski and Stevens, 2001). This is the "one-site, one-vesicle" hypothesis. It also has been suggested that, in some circumstances, more than one vesicle can be released from a single synapse following a stimulus, a hypothesis termed multivesicular release (MVR) (Tong and Jahr, 1994; Auger et al., 1998; Prange and Murphy, 1999). These two hypotheses lead to different predictions. The one-site, one-vesicle hypothesis suggests that event-to-event changes in the transmitter concentration transient in the cleft result from either differences in vesicular filling or the rate at which exocytosis occurs. The MVR hypothesis, however, adds the more dramatic method of altering the transmitter transient by varying the number of packets of transmitter released. Assuming the simplest model of MVR, in which each vesicle is released independently, the likelihood of multiple exocytotic events at a single release site would increase with the probability of release (P_r).

[1]Correspondence: jahr@ohsu.edu

Evidence for the one-site, one-vesicle hypothesis comes from combined morphological and electrophysiological studies suggesting that the number of morphologically defined synaptic contacts exceeds the number of quanta released by a presynaptic stimulus (Redman, 1990; Korn et al., 1994). This is interpreted to mean that release at each site is limited to a single vesicle. On the other hand, MVR clearly occurs at the neuromuscular junction, at least at artificially high release probabilities (Heuser et al., 1979). In addition, at single inhibitory synapses in the cerebellum, MVR was observed as the nonlinear summation of postsynaptic currents following presynaptic stimulation (Auger et al., 1998). MVR has also been reported at the excitatory synapses of cultured hippocampal neurons (Tong and Jahr, 1994). By using low-affinity competitive antagonists of NMDA receptors (Clements et al., 1992), Tong and Jahr (1994) found that larger glutamate concentration transients occurred in the cleft in conditions of high P_r than of low P_r. This was interpreted as evidence for MVR. However, it has been suggested that these data from excitatory synapses could be explained by the pooling of glutamate released from adjacent sites (Barbour and Hausser, 1997; Rusakov and Kullmann, 1998; Auger and Marty, 2000). In this interpretation, high P_r conditions lead to an increased likelihood that adjacent synapses release simultaneously following a stimulus. If glutamate can readily diffuse from one synapse to its neighbors (Barbour and Hausser, 1997; Rusakov and Kullmann, 1998), higher cleft concentrations will occur when adjacent synapses release simultaneously than when only one releases. Qualitatively, the low-affinity antagonist technique by itself will not distinguish between these two interpretations.

The climbing fiber-Purkinje cell (CF-PC) synapse in the cerebellar cortex is well suited for studying whether MVR occurs during normal synaptic transmission. Each Purkinje cell receives input from a single climbing fiber, but this input is extremely strong, consisting of approximately 500 individual synapses (Palay and Chan-Palay, 1974). Climbing fiber stimulation results in very large excitatory postsynaptic currents (EPSCs) in Purkinje cells, both because of the number of synapses and because the average P_r at these synapses is very high (Silver et al., 1998; Dittman and Regehr, 1998). Because of this high P_r, MVR should occur frequently at CF-PC synapses if there is no mechanism to prevent it. Another consequence of having synapses with high P_r is that neighboring synapses will likely release glutamate to the same stimulus. As glutamate can diffuse out of the synaptic cleft (Bergles et al., 1997; Clark and Barbour, 1997), pools of glutamate from neighboring synapses could interact, thereby increasing synaptic concentrations and slowing clearance (Otis et al., 1996). The specialized architecture of the CF-PC synapse may limit the extent of interaction of glutamate released at neighboring synapses. Unlike synapses in the cerebral cortex and hippocampus (Spacek, 1985; Ventura and Harris, 1999), CF-PC synapses are almost entirely covered by sheets of Bergmann glial membranes (Palay and Chan-

Palay, 1974; Spacek, 1985; Xu-Friedman et al., 2001). In addition, each glial-encased Purkinje cell spine contacted by a climbing fiber makes a single, morphologically defined synapse (Xu-Friedman et al., 2001). Furthermore, Bergmann glial membranes and perisynaptic regions of Purkinje cell spines express very high densities of glutamate transporters, ~5400 per μm^2 (Lehre and Danbolt, 1998) and 1800 per μm^2 (Dehnes et al., 1998), respectively. Both the physical barrier to diffusion provided by the enveloping Bergmann glial membranes and the chemical barrier of glutamate transporters decrease the likelihood of spillover and pooling, and will therefore tend to isolate individual synapses.

In the present study, the glutamate concentration transient at CF-PC synapses was estimated by analyzing the nonequilibrium inhibition of postsynaptic AMPA receptors by a low-affinity competitive antagonist. We suggest that the peak concentration of glutamate at an average release site correlates with the P_r but is not affected by spillover or pooling of glutamate released from neighboring synapses. We propose that the elevated concentrations of glutamate necessary to account for the results arise from the concomitant release of multiple vesicles per site per stimulus.

Results

Climbing Fiber-Evoked EPSCs

Synaptic transmission at CF-PC synapses was studied at 32°C–35°C with whole-cell patch recordings from visually identified Purkinje cells in cerebellar slices from young rats (P11-17). Climbing fiber stimulation results in large, all-or-none EPSCs in Purkinje cells that are mediated by AMPA receptors (e.g., Konnerth et al., 1990). The amplitude of the second EPSC (EPSC2) of a pair stimulated at a 50 ms interval was 57.1% ± 10.7% ($n = 7$) of the first EPSC (EPSC1) (Figure $1A_1$). This paired-pulse depression results from a long-lasting lowered P_r following the first stimulus (Dittman and Regehr, 1998; Hashimoto and Kano, 1998; Silver et al., 1998). EPSC1 and EPSC2 had different kinetics. EPSC1 had a faster rise time than EPSC2 but decayed significantly more slowly (Table 1). The decay phases of both EPSC1 and EPSC2 were well described by a sum of two exponentials. The main difference in the decays of the two EPSCs was that the fast component of EPSC1 was smaller than that of EPSC2 (47.3% versus 73.3%, respectively; Table 1).

P_r Determines Glutamate Concentration at the Synaptic Cleft

To determine whether a decrease in P_r results in a smaller glutamate concentration transient at individual synapses, we compared the inhibition of EPSC1 and EPSC2 caused by a low-affinity competitive antagonist of AMPA receptors. The rationale for these experiments is based on the nonequilibrium interaction between the transient presence of glutamate and the continuous presence of antagonist (Clements et al., 1992; Clements, 1996). If a competitive antagonist remains bound to the receptor for a period that is similar to or shorter than the period that glutamate is present, some of the receptors that are bound by the antagonist at the instant of neurotransmitter release will become available for glutamate binding, or rebinding by antagonist, during the glutamate transient. Thus, the amount of inhibition of the EPSC will depend not only on the concentration of the antagonist, but also on the amplitude and time course of the glutamate transient. In contrast, if an antagonist with a very long bound time is used, only those receptors that are unoccupied by antagonist at the instant of release will be able to bind glutamate, because very few receptors will unbind antagonist during the relatively short presence of glutamate. In this case, then, inhibition of the EPSC will depend only on the concentration of antagonist, and changes in the glutamate transient will be ineffective.

The low-affinity competitive antagonist γ-D-glutamylglycine (γ-DGG; 2 mM) (Watkins, 1991; Liu et al., 1999) inhibited EPSC2 more than EPSC1 (Figures $1A_1$ and $1A_2$; 26.9% ± 6.1% block of EPSC1 versus 54.2% ± 6.0% block of EPSC2, $n = 7$, $p < 0.0001$; Figure 1D), suggesting that a smaller glutamate transient resulted from the second stimulus. In addition, the rise time of EPSC1 was slowed in the presence of γ-DGG (Figure $1A_2$ inset and Table 1; $p < 0.006$, paired t test; $n = 7$). This slowing is consistent with the requirement for γ-DGG to unbind from AMPA receptors before glutamate can bind and activate them. A similar effect was also seen for EPSC2 (see Table 1). γ-DGG also accelerated the decay of EPSC1 (Figure $1A_2$). This faster decay of EPSC1 in γ-DGG suggests that the slow tail current in control results from low concentrations of glutamate with which γ-DGG competes more effectively than the higher glutamate concentrations present at the peak of EPSC1. Apparently, the decay rate of EPSC1 is limited by the slow clearance of glutamate (Barbour et al., 1994) rather than AMPA receptor channel kinetics. As the time course of EPSC2 did not change in the presence of γ-DGG (Table 1), we suggest that clearance of glutamate is faster following the second stimulus, possibly because transporters are not as close to saturation as they are following the first stimulus.

To further constrain the simulations (see below) and to test the generality of the result, we measured the inhibition of the EPSCs by 1 mM γ-DGG or by 1 mM kynurenate. Qualitatively, the differential inhibition of EPSC1 and EPSC2 and the changes in EPSC time course were the same as with 2 mM γ-DGG. EPSC1 and EPSC2 were inhibited by 17.4% ± 1.0% and 31.1% ± 5.9% by 1 mM γ-DGG ($n = 4$) and 38.7% ± 8.0% and 65.2% ± 2.1% by 1 mM kynurenate ($n = 3$).

Following washout of γ-DGG, each cell was tested with a low concentration of the slowly unbinding antagonist NBQX (100 nM) (Figures 1B and 1C). NBQX inhibited both EPSCs to the same extent (Figure 1D; 53.0% ± 9.6% and 54.8% ± 10.0% of control; $n = 7$) and did not alter either their rise or decay times (Figure $1B_2$ inset and Table 1), indicating that the differential block and alteration of time course of the EPSCs by γ-DGG was not the result of voltage escape.

Although attenuation of synaptic currents by voltage escape was assessed by application of the high-affinity blocker NBQX, dendritic filtering of synaptic responses might alter the time course of the CF-PC EPSCs as recorded at the soma. A voltage-jump protocol was used to determine the time course of the synaptic conduc-

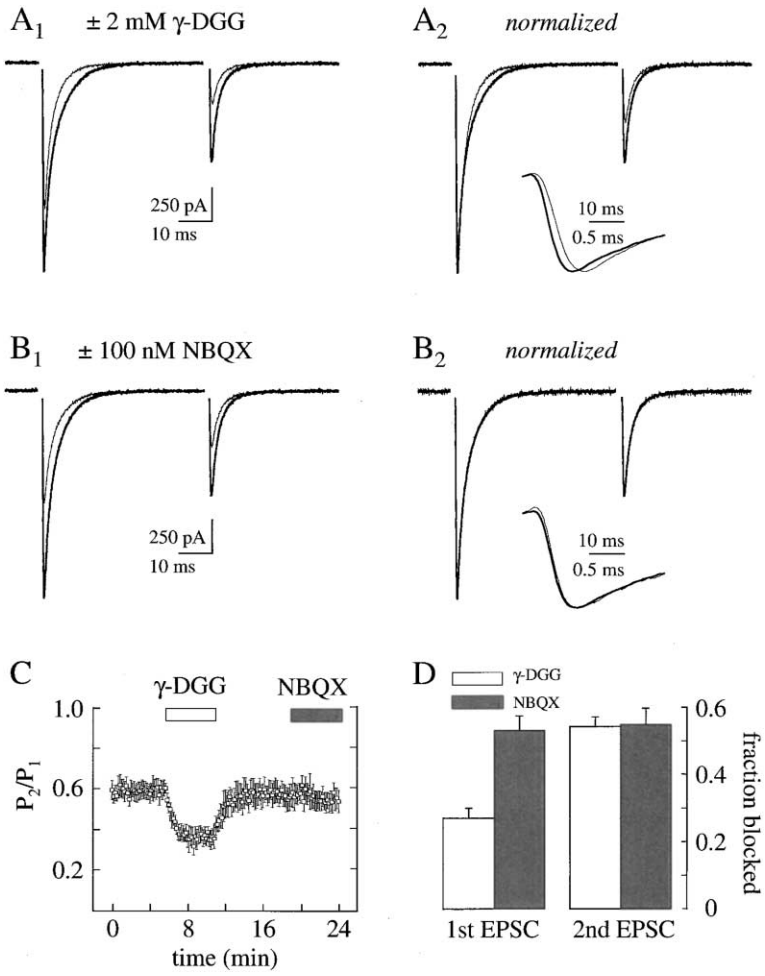

Figure 1. Inhibition of Paired CF-PC EPSCs by γ-DGG and NBQX

(A_1) Superimposed CF-PC EPSCs in control (thick line) and in 2 mM γ-DGG, paired at 50 ms intervals in 2.5 mM Ca^{2+}.

(A_2) Responses in (A_1) normalized to the peak of the first EPSC; (inset) the rising phases of the first EPSCs in (A_2).

(B_1) NBQX (100 nM) inhibits both EPSCs equally (thick line, control).

(B_2) Responses in (B_1) normalized to the peak of the first EPSC; (inset) rising phase of the first EPSCs in (B_2) (same cell as in [A]).

(C) Time course of paired-pulse inhibition for a group of cells (n = 7).

(D) Summary of inhibition of EPSCs in 2 mM γ-DGG (open bar) and 100 nM NBQX (filled bar; n = 7 for each). All traces are averages of 4–10 responses.

tance that generates the CF-EPSC (Pearce, 1993; Hausser and Roth, 1997). The principle of the technique is that a voltage jump that increases the driving force will alter synaptic charge transfer only if the voltage jump occurs while the synaptic conductance is active (Hausser and Roth, 1997). The decay time course of the conductances generating EPSC1 and EPSC2 was estimated using an analytical function (Hausser and Roth, 1997) in which the exponential time constant for charging the membrane and the decay of the conductance were allowed to vary. Two time constants were needed to fit the charge recovery curve (data not shown; n = 5). The average time constants of the decay of the synaptic conductance for EPSC1 obtained by fitting the charge-recovery curves were 1.3 ± 0.7 ms (57.4% ± 25%) and 5.0 ± 0.9 ms (data not shown; n = 5), whereas EPSC2 had time constants of 1.0 ± 0.4 ms (80.9% ± 14.6%) and 6.9 ± 2.8 ms (data not shown; n = 3). These data are not significantly different from the time constants needed to fit the EPSCs recorded using a somatic recording electrode. This indicates that the slow decay of the CF-PC EPSC does not result from dendritic filtering.

P_r Determines Inhibition by γ-DGG

Differences in the size of the glutamate transients activating EPSC1 and EPSC2 could result from MVR, that is, more than one vesicle released per synapse per presynaptic action potential, or by spillover and pooling of glutamate released from neighboring synaptic connections (Tong and Jahr, 1994; Rusakov and Kullmann, 1998; Auger and Marty, 2000). If these mechanisms are only decreased but not eliminated during EPSC2, further reductions in P_r should result in greater EPSC inhibition by γ-DGG, but not by NBQX.

Table 1. EPSC Parameters in 2.5 mM Ca^{2+} (n = 7)

	EPSC1			EPSC2		
	Control	γ-DGG (2 mM)	NBQX (100 nM)	Control	γ-DGG (2 mM)	NBQX (100 nM)
Rise times (ms)	0.22 ± 0.04	0.27 ± 0.05	0.22 ± 0.03	0.30 ± 0.06	0.35 ± 0.07	0.29 ± 0.02
Decay time fast (ms)	1.2 ± 0.6	1.7 ± 0.6	1.7 ± 1.1	1.7 ± 0.6	1.9 ± 0.5	2.1 ± 0.3
% fast	47.3 ± 23.5	59.6 ± 22.2	52.3 ± 30.0	73.3 ± 9.9	84.1 ± 4.0	81.5 ± 10.4
Decay time slow (ms)	5.6 ± 0.6	5.5 ± 1.1	6.6 ± 2.2	5.5 ± 1.5	8.0 ± 2.1	7.7 ± 1.5

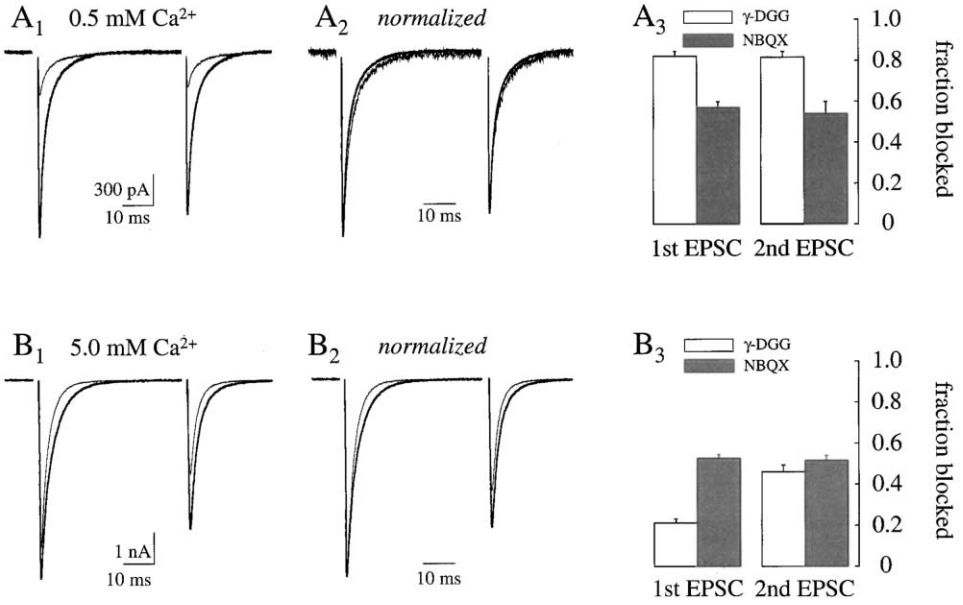

Figure 2. Lowering P_r Increases Inhibition by γ-DGG but Not by NBQX

(A_1) Superimposed CF-PC EPSCs in control (thick line) and in 2 mM γ-DGG, paired at 50 ms intervals in 0.5 mM external Ca^{2+}.

(A_2) Response in (A_1) normalized to the peak of the first EPSC.

(A_3) Summary of inhibition of EPSCs in 2 mM γ-DGG (open bar) and 100 nM NBQX in 0.5 mM Ca^{2+} (filled bar; n = 7).

(B_1) Superimposed evoked EPSCs (as in [A]) in control (thick line) and in 2 mM γ-DGG, both in 5 mM Ca^{2+}.

(B_2) EPSCs in (B_1) scaled to the peak of the first EPSC.

(B_3) Summary of inhibition of EPSCs in 2 mM γ-DGG (open bar) and 100 nM NBQX in 5 mM Ca^{2+} (filled bar; n = 4 for each). For each recording condition, both γ-DGG and NBQX were always applied to each cell with a washout in between drug applications.

Lowering extracellular Ca^{2+} from 2.5 to 0.5 mM (and increasing Mg^{2+} from 1.3 to 3.3 mM) reduced EPSC1 to 40.7% ± 13% of its control value and EPSC2 to 58.6% ± 19% (n = 3) (see also Silver et al., 1998; Dittman and Regehr, 1998), and thus resulted in an increase in the paired-pulse ratio of the two EPSCs (0.9 ± 0.1, n = 5; Figure 2A). Both EPSCs decayed with similar kinetics that were faster than EPSC1 in 2.5 mM Ca^{2+} (Table 2). Application of γ-DGG (2 mM) to EPSCs evoked in 0.5 mM Ca^{2+} caused a greater block of both EPSCs (82.0% ± 6.5% and 81.5% ± 6.7%, respectively, n = 7; Figures $2A_1$–$2A_3$) but had no significant effect on their decay times (Figure $2A_2$ and Table 2). In contrast, the slowly dissociating antagonist NBQX blocked both EPSCs to the same extent as in 2.5 mM Ca^{2+} (57.0% ± 4.5% and 54.2% ± 5.4%; n = 5; Figure $2A_3$) without any change in kinetics. These data suggest that the glutamate transient sensed by AMPA receptors in low P_r conditions is smaller than the transient in 2.5 mM Ca^{2+}.

When P_r was decreased further by increasing Mg^{2+} to 10 mM (with 0.5 mM Ca^{2+}), no additional inhibition by γ-DGG was observed. In this recording solution, paired pulse facilitation occurred (EPSC2/EPSC1 = 1.4 ± 0.1, n = 5), indicating that P_r was lower than in 0.5 mM Ca^{2+} and 3.3 mM Mg^{2+}; however, the time course of the EPSCs was not changed (data not shown, n = 5). γ-DGG (2 mM) inhibited both EPSCs equally (80.0% ± 3.0% and 78.1% ± 4.9%, n = 5). These data suggest that in both low P_r conditions tested, the average glutamate concentration transient at active synapses was the same and had reached a minimum, indicating that neither MVR nor glutamate pooling occurred in either condition.

Increasing external Ca^{2+} from 2.5 to 5 mM did not significantly alter the amplitudes of EPSC1 or EPSC2 (101.9% ± 4.1% and 98.5% ± 3.1%, respectively, n = 4). In 5 mM Ca^{2+}, γ-DGG (2 mM) inhibited EPSC1 by 17.8% ± 4.3% and EPSC2 by 45.7% ± 5.8%, less than the inhibition in 2.5 Ca^{2+} (p = 0.03 and p = 0.05, respectively, n = 4; Figures $2B_1$–$2B_3$ and Table 3). Despite the lack of change in EPSC amplitude, these results suggest

Table 2. EPSC Parameters in 0.5 mM Ca^{2+} (n = 5)

	EPSC1			EPSC2		
	Control	γ-DGG (2 mM)	NBQX (100 nM)	Control	γ-DGG (2 mM)	NBQX (100 nM)
Rise times (ms)	0.24 ± 0.05	0.26 ± 0.08	0.26 ± 0.06	0.24 ± 0.06	0.30 ± 0.06	0.25 ± 0.06
Decay time fast (ms)	1.2 ± 0.7	1.4 ± 0.6	1.3 ± 0.6	1.2 ± 0.5	1.3 ± 0.7	1.3 ± 0.4
% fast	61.7 ± 21.9	64.8 ± 24.4	65.2 ± 23.6	57.8 ± 24.7	57.8 ± 36.6	68.3 ± 22.9
Decay time slow (ms)	4.2 ± 1.2	5.5 ± 2.3	4.9 ± 2.3	3.9 ± 1.0	5.8 ± 3.3	5.9 ± 0.9

Table 3. EPSC Parameters in 5 mM Ca^{2+} (n = 4)

	EPSC1			EPSC2		
	Control	γ-DGG (2 mM)	NBQX (100 nM)	Control	γ-DGG (2 mM)	NBQX (100 nM)
Rise times (ms)	0.22 ± 0.03	0.26 ± 0.01	0.22 ± 0.04	0.33 ± 0.04	0.35 ± 0.05	0.31 ± 0.01
Decay time fast (ms)	1.8 ± 0.5	2.1 ± 0.6	2.7 ± 2.0	2.0 ± 0.4	2.1 ± 0.4	2.2 ± 0.4
% fast	42.9 ± 27.1	62.9 ± 33.0	64.4 ± 33.8	84.9 ± 11.1	92.9 ± 6.6	92.4 ± 7.5
Decay time slow (ms)	5.0 ± 0.3	4.1 ± 0.3	3.7 ± 0.3	9.0 ± 4.5	6.2 ± 1.5	4.8 ± 0.4

that the peak glutamate concentration can be further elevated at CF-PC synapses in 5 mM Ca^{2+} and implies that in both concentrations of Ca^{2+} (2.5 and 5 mM), AMPA receptors contributing to the peak amplitude of EPSC1 are saturated (see Silver et al., 1998).

Blockade of Glutamate Transport

Either MVR release from individual synapses or pooling of glutamate from adjacent synapses could, at least qualitatively, explain the results discussed previously. As both Bergmann glial cells, which surround Purkinje cell dendrite spines (Palay and Chan-Palay, 1974; Spacek, 1985; Xu-Friedman et al., 2001), and Purkinje cells express high densities of glutamate transporters (Lehre and Danbolt, 1998; Dehnes et al., 1998), spillover and pooling of glutamate between neighboring synapses should be enhanced if transport is inhibited. If the differential inhibition of EPSCs at different release probabilities results from pooling, inhibition of glutamate transporters should increase the glutamate transient and decrease the inhibition of the EPSC by γ-DGG. The competitive antagonist of glutamate transport, DL-threo-β-benzyloxyaspartate (TBOA, 30 μM) (Shimamoto et al., 1998), slowed the decay of both EPSC1 and EPSC2 without changing the holding current, which is consistent with the role of transport in clearing the glutamate transient (Figure 3A) (Barbour et al., 1994). In the same cells, the fast component of decay of EPSC1 was not changed in the presence of TBOA (Table 4). However, the slow time constant nearly doubled ($p < 0.002$; Table 4). Despite this slowing of clearance and the presumed exacerbation of pooling in the presence of TBOA, γ-DGG (2 mM) blocked both EPSC1 and EPSC2 to the same extent as in the absence of TBOA (27.7% ± 2.9% and 50.8% ± 3.0%, respectively, n = 4; Figures 3B and 3C). The prolongation of the decay of the EPSCs by TBOA results from slowed clearance and presumably diffusion to more distant AMPA receptors than in normal conditions. However, the lack of effect of TBOA on the peak EPSC inhibition by γ-DGG indicates that the P_r-

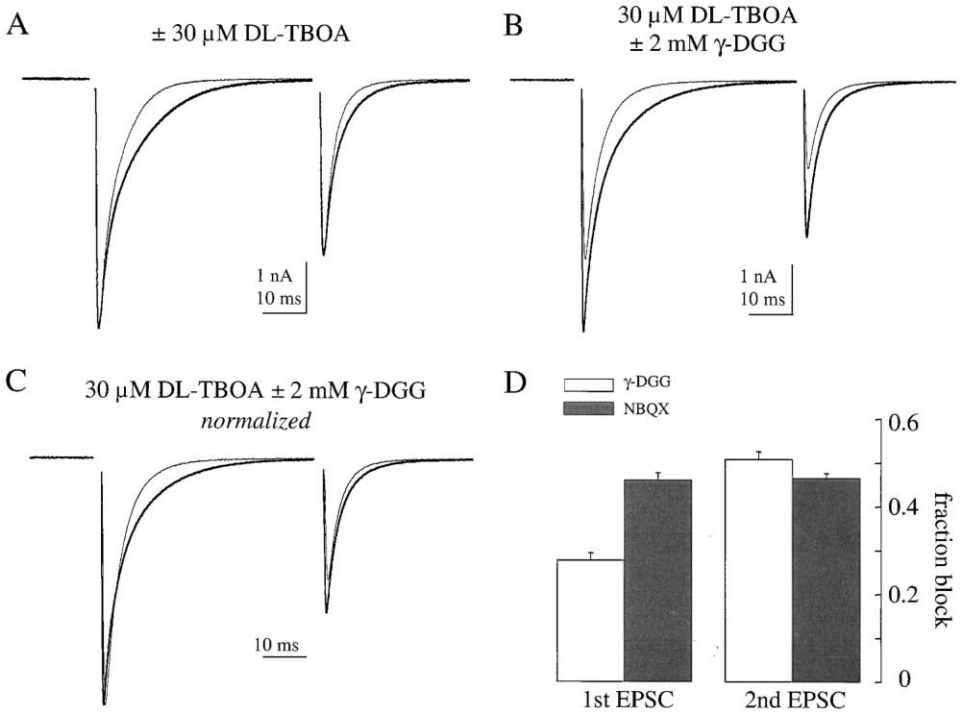

Figure 3. EPSC Inhibition Is Unaffected by the Glutamate Uptake Antagonist TBOA

(A) Superimposed CF-PC EPSCs in control (thin line) and in the presence of 30 μM TBOA (thick line).

(B) Superimposed CF-PC EPSCs in the presence of 30 μM TBOA (thick line) and TBOA plus 2 mM γ-DGG (thin line).

(C) Responses in (B) normalized to the peak of the first EPSC.

(D) Summary of inhibition of EPSCs in the presence of TBOA plus γ-DGG (open bar) or 100 nM NBQX (filled bar; n = 4 for each).

Table 4. EPSC Parameters in 2.5 mM Ca^{2+} and 30 μM TBOA (n = 5)

	EPSC1			
	Control (no TBOA)	Control (TBOA)	γ-DGG (2 mM)	NBQX (100 nM)
Rise times (ms)	0.23 ± 0.02	0.23 ± 0.02	0.29 ± 0.02	0.22 ± 0.06
Decay time fast (ms)	0.9 ± 0.2	1.3 ± 0.5	2.4 ± 0.7	1.5 ± 0.4
% fast	28.2 ± 15.1	41.9 ± 13.2	59.9 ± 23.2	50.2 ± 3.9
Decay time slow (ms)	4.3 ± 0.8	7.8 ± 1.5	6.3 ± 0.5	9.3 ± 1.5
	EPSC2			
	Control (no TBOA)	Control (TBOA)	γ-DGG (2 mM)	NBQX (100 nM)
Rise times (ms)	0.29 ± 0.04	0.29 ± 0.04	0.36 ± 0.02	0.29 ± 0.08
Decay time fast (ms)	1.7 ± 0.5	1.6 ± 0.4	2.1 ± 0.38	1.6 ± 0.36
% fast	72.5 ± 13.2	52.4 ± 6.8	73.0 ± 20.0	62.6 ± 6.2
Decay time slow (ms)	4.6 ± 0.9	5.3 ± 0.7	5.6 ± 1.1	6.2 ± 0.8

induced changes in the early part of the glutamate transient that are responsible for the peak amplitude of the EPSC do not result from pooling of glutamate.

γ-DGG Does Not Alter Release

Manipulations that change P_r alter synaptic facilitation and depression (del Castillo and Katz, 1954). Because γ-DGG, but not NBQX, increased paired-pulse depression in 2.5 mM Ca^{2+} (Figure 1C), we tested, by recording the synaptically activated transport current (STC) in Purkinje cells, whether γ-DGG affects the release of glutamate from climbing fiber terminals (Otis et al., 1997; Auger and Attwell, 2000). The STC was recorded in the absence of permeable anions, in which condition the STC is carried by the cotransport of 3 Na^+, 1 H^+, and 1 glutamate and the countertransport of 1 K^+ (Zerangue and Kavanaugh, 1996; Bergles and Jahr, 1997; Auger and Attwell, 2000). After activation of the climbing fiber-stimulated AMPA receptor EPSC, high concentrations of AMPA receptor antagonists (25 μM NBQX) were added to the recording solution to isolate the STC (Otis et al., 1997; Auger and Attwell, 2000). The addition of 2 mM γ-DGG had no effect on the amplitudes or kinetics of STCs evoked by climbing fiber stimuli paired at 50 ms intervals (STC1, 98.1% ± 12.7% of control amplitude; STC2, 99.6% ± 15.0% of control amplitude; paired-pulse ratio in control, 0.4 ± 0.09; in γ-DGG, 0.39 ± 0.07; n = 7; Figure 4). Similar results were obtained when using the transporter-permeant anion NO_3^- as the internal anion (n = 4; data not shown) (Wadiche et al., 1995; Eliasof and Jahr, 1996; Otis et al., 1997; Wadiche and Kavanaugh, 1998; Auger and Attwell, 2000). These data indicate that γ-DGG does not alter the release of glutamate at CF-PC synapses and that its effect on paired-pulse depression of the EPSC is the result of its actions on postsynaptic AMPA receptors.

Kinetic Model

A kinetic model of the Purkinje cell AMPA receptor was developed to estimate the changes in the glutamate transient at CF-PC synapses over the range of P_rs tested experimentally (Figure 5) (Clements et al., 1992; Diamond and Jahr, 1997). The model was based on Hausser and Roth (1997) but was modified to fit responses of outside-out patches to glutamate applications at 32°C–35°C. Four types of experiments were performed. Paired-pulse recovery experiments using pulses of 10 mM glutamate were used to determine the rates of AMPA receptor deactivation, desensitization, and recovery from desensitization (Figures 6A and 6B). The time constant of recovery was 16.9 ± 1.0 ms (n = 6). The desensitization rate during a 20 ms pulse of 10 or 50 mM glutamate had a time constant of 2.3 ± 0.3 ms (n = 6). Two further experiments were performed to estimate the relative binding and unbinding rates of glutamate and γ-DGG. First, pulses of 10 mM glutamate were applied to patches in control conditions and after preequilibration with 2 mM γ-DGG (Figure 6C). This experiment was designed to test the unbinding rate of γ-DGG. Preequilibration with 2 mM γ-DGG resulted in a reduction of the peak current amplitude to 74.5% ± 4.6% (n = 12) of control values (10 mM glutamate alone). In addition, the rising phase of the current was markedly slowed in the presence of γ-DGG (20%–80% rise time, 0.13 ± 0.05 ms and 0.23 ± 0.08 ms, control and γ-DGG, respectively, $p < 0.002$, n = 12). Second, patch responses to applications of equal concentrations of glutamate and γ-DGG were compared with pulses of glutamate alone (Figure 6D). This experiment was used to estimate the relative binding rates of P_r and L-glutamate.

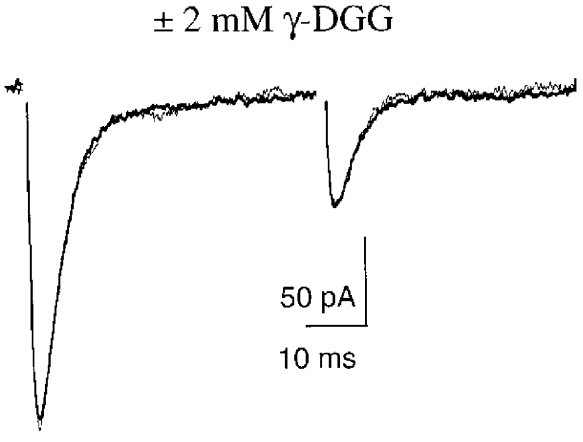

Figure 4. Synaptic Transporter Current Is Not Affected by γ-DGG

Superimposed synaptic transporter currents in a Purkinje cell evoked by CF stimulation in the presence of 25 μM NBQX ± 2 mM γ-DGG (γ-DGG, thin line) paired at 50 ms intervals.

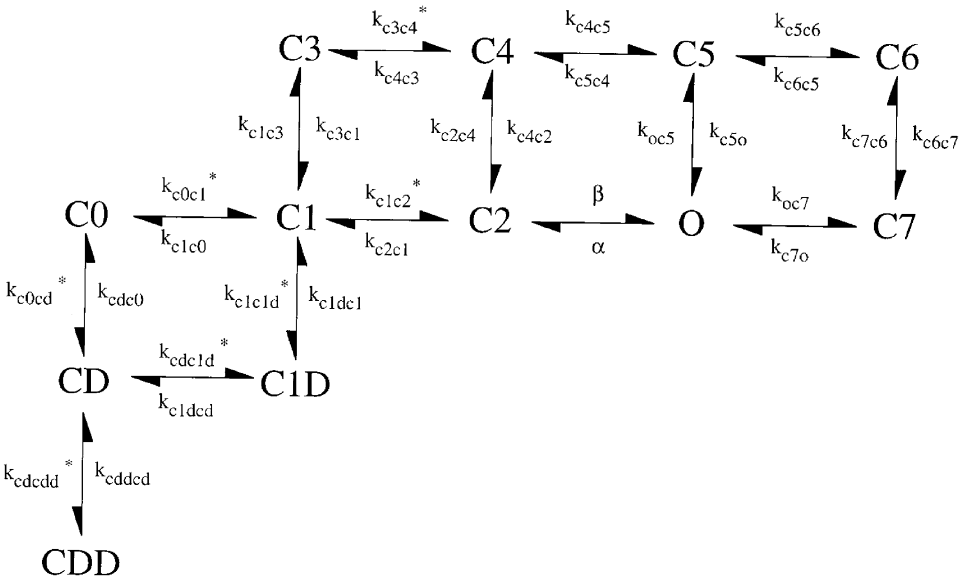

Figure 5. AMPA Receptor Model

Kinetic scheme of the AMPA receptor model used to fit AMPA receptor currents in outside-out patches. Rates were as follows (units are M^{-1} s^{-1} for rates denoted by * or s^{-1}) $k_{c0c1} = 1.366 \times 10^7$, $k_{c1c0} = 2.0393 \times 10^3$, $k_{c1c2} = 6.02 \times 10^6$, $k_{c2c1} = 4.72 \times 10^3$, $\beta = 1.72 \times 10^4$, $\alpha = 3.73 \times 10^3$, $k_{oc7} = 1.14 \times 10^2$, $k_{c7o} = 9.05 \times 10^1$, $k_{c1c3} = 4.22 \times 10^2$, $k_{c3c1} = 1 \times 10^2$, $k_{c2c4} = 2 \times 10^3$, $k_{c4c2} = 4.67 \times 10^1$, $k_{oc5} = 3.11$, $k_{c5o} = 6.92 \times 10^{-1}$, $k_{c7c6} = 2.99$, $k_{c6c7} = 3.242 \times 10^{-1}$, $k_{c3c4} = 1.37 \times 10^7$, $k_{c4c3} = 1.054 \times 10^3$, $k_{c4c5} = 4.76 \times 10^2$, $k_{c5c4} = 9.84 \times 10^2$, $k_{c5c6} = 1.034 \times 10^4$, $k_{c6c5} = 4 \times 10^3$, $k_{c0cd} = 2 \times 10^7$, $k_{cdc0} = 1.01 \times 10^4$, $k_{cdcdd} = 5 \times 10^7$, $k_{cddcd} = 1.47 \times 10^5$, $k_{cdc1d} = 1 \times 10^4$, $k_{c1dcd} = 4.992 \times 10^{-3}$, $k_{c1c1d} = 2.28 \times 10^6$, $k_{c1dc1} = 3.85$. Rates k_{c0c1}, k_{c1c2}, k_{c3c4}, and k_{cdc1d} are dependent on [glutamate], whereas k_{c0cd}, k_{cdcdd}, and k_{c1c1d} are dependent on [γ-DGG].

Applications of glutamate alone and those with γ-DGG were interleaved to control for rundown. By altering the values of the rate constants (Figure 5), the model accurately reproduced control responses to exogenously applied glutamate as well as the effects of γ-DGG observed in the patch experiments described previously in this article. Finally, nonstationary noise analysis was performed on outside-out patch responses to 10 mM glutamate to estimate the maximum open probability (P_o) of AMPA receptors at 32°C–35°C (Sigworth, 1980). The maximum P_o obtained by this method was 0.66 ± 0.05 (n = 7).

Synaptic Glutamate Transient

We have estimated the glutamate concentration transient presented to AMPA receptors by synaptic release by challenging the kinetic model with simulated glutamate transient-driving functions in control conditions and in the presence of γ-DGG. The EPSC evoked in 0.5 mM Ca^{2+} was simulated first because it is likely the sum of synaptic activity resulting from the release of single vesicles at individual synapses. However, the glutamate transient required to simulate the low-calcium EPSC waveform and allow 2 mM γ-DGG to block by ~80% resulted in a simulated EPSC with a decay phase that was accelerated by the addition of γ-DGG (Figure 7A). Such an acceleration was not seen in the experimental data (Figure $2A_2$). This indicates that the decay of the AMPA receptor conductance at active synapses in 0.5 mM Ca^{2+} was not determined by slow clearance of glutamate but rather by channel kinetics and that the simulated glutamate transient did not mimic the true transient. In addition, the decay phases of both the experimental and simulated EPSC were slower than the deactivation of AMPA receptor currents in outside-out patches (see below), suggesting that the EPSC in 0.5 mM Ca^{2+} might decay more slowly than the underlying unitary events at individual synapses. Release asynchrony across release sites and dendritic filtering could both contribute to a slower decay phase. To estimate the contribution of release asynchrony, we recorded single quantal EPSCs evoked by CF stimulation in the presence of 0.5 mM Sr^{2+} in the absence of Ca^{2+} (Alvarez-Leefmans et al., 1979; Goda and Stevens, 1994; Abdul-Ghani et al., 1996; Otis et al., 1997). These asynchronous EPSCs evoked in Sr^{2+} (aEPSCs), occurring between 50 and 300 ms following the stimulus, were aligned by their rising phases and averaged (Figure 7B). The averaged aEPSCs had rise and decay times that were similar to those seen in outside-out patches and faster than those of the low-calcium EPSC. aEPSCs decayed with two exponentials: 0.4 ± 0.2 ms (42% ± 10%) and 2.2 ± 0.8 ms (n = 5), whereas the deactivation phase of patch currents was well fitted with a single exponential of 1.3 ± 0.3 ms (n = 18). The weighted, single exponential decay of aEPSCs was 1.46 ± 0.53 ms (n = 5), similar to the patch decay time. The model was used to obtain an estimate of the glutamate transient necessary to simulate the aEPSC (see below). The simulated waveform of the aEPSC was deconvolved from that of the low-calcium EPSC to obtain an estimate of the time course of release asynchrony (Figure 7C). This waveform indicates that 67% of release is completed in 0.75 ms. Thus, although the variability of synaptic delay is brief, it adds significantly to the low-calcium EPSC time course and corrupts the simulation of the glutamate transient. We have therefore used the

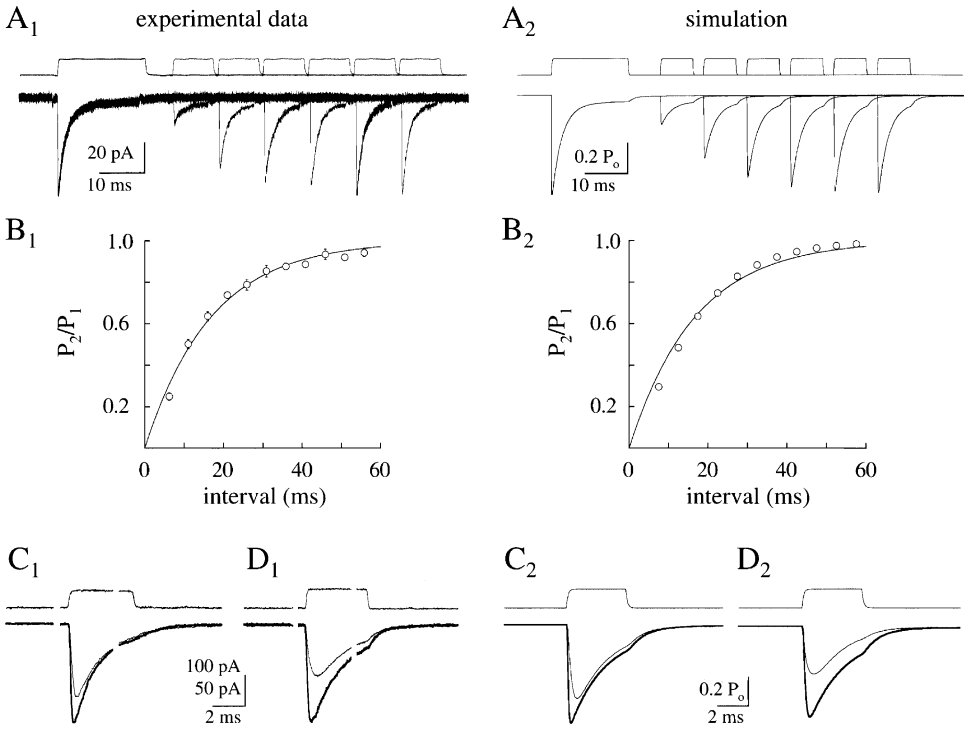

Figure 6. AMPA Receptor Currents in Outside-Out Patches and Simulations

(A_1) Time course of AMPA receptor recovery from desensitization. Superimposition of seven average traces from an outside-out somatic patch exposed to one 20 ms and one 10 ms application of 10 mM glutamate separated by different intervals.

(A_2) Simulated paired-pulse recovery from desensitization as in (A_1).

(B_1) Recovery curve from desensitization expressed as the ratio of second peak (P_2) as a function of the first peak (P_1) for six patches.

(B_2) Recovery curve from desensitization for simulated currents as in (B_1).

(C_1) Superimposed traces activated by 4 ms application of 10 mM glutamate in the absence (thick line) and presence of 2 mM γ-DGG.

(C_2) Simulated displacement experiment as in (C_1).

(D_1) Superimposed traces activated by 4 ms application of 2 mM glutamate (thick line) or 2 mM glutamate with 2 mM γ-DGG.

(D_2) Simulated experiment as in (D_1).

aEPSC time course in simulations to estimate the single quantal glutamate transient.

Simulated glutamate transients had to fit the kinetics of the aEPSC as well as the amount of inhibition of the 0.5 mM Ca^{2+} EPSC by γ-DGG (assuming that each active synapse contributing the 0.5 mM Ca^{2+} EPSC was independent and released a single vesicle, i.e., negligible pooling and MVR). At the peak of the aEPSC, P_o was

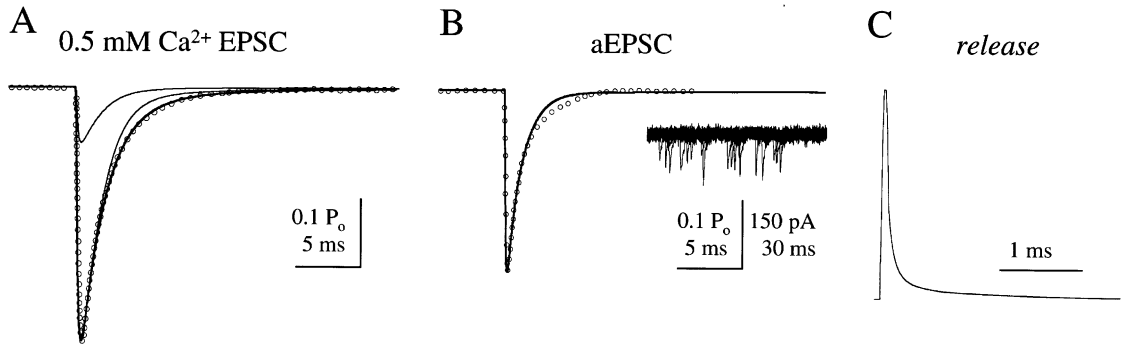

Figure 7. Release Asynchrony

(A) Superimposed CF-PC EPSC in 0.5 mM Ca^{2+} (dotted line), the simulation used in the deconvolution (thick line, slow decay), the simulation in γ-DGG (thin line, small response), and γ-DGG simulation normalized to peak amplitude (thin line, faster decay).

(B) Superimposed averaged Sr^{2+}-evoked aEPSC (dotted line; 0.5 mM Sr^{2+}) and the simulation (thick line) used in the deconvolution. Inset: raw aEPSC.

(C) Time course of vesicle release in 0.5 mM Ca^{2+}. Sr^{2+}-evoked aEPSC simulation in (B) was deconvolved from the CF-PC EPSC simulation in 0.5 mM Ca^{2+} in (A).

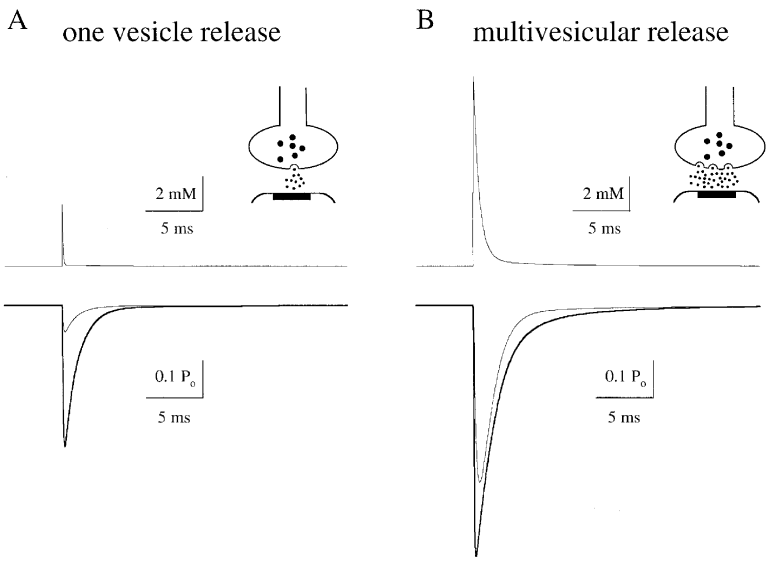

Figure 8. Simulated EPSC in Low and Normal P_r and Respective Synaptic Glutamate Transient

(A) Simulated EPSCs (bottom) in the absence (thick line) and presence of 2 mM γ-DGG driven by the glutamate transient (top) in conditions to mimic 0.5 mM Ca^{2+}.

(B) Same as in (A), but in conditions mimicking 2.5 mM Ca^{2+}.

estimated to range from 0.27 to 0.39. The lower limit peak P_o of 0.27 was calculated from the nonstationary noise estimate of peak P_o in patches (0.66) and 59% diminution of the EPSC amplitude accompanying a change in Ca^{2+} from 2.5 to 0.5 mM ($0.66 \times 0.41 = 0.27$). This is a lower limit, as some synapses likely do not release following action potential invasion at 0.5 mM Ca^{2+}. The upper limit (0.39) was the highest that allowed γ-DGG to inhibit the simulated aEPSC by 82%. We chose a peak P_o of 0.38 for illustration (Figure 8A). The best fit of the aEPSC was obtained with a glutamate transient that rose to a peak of 3.7 mM, with a rise time of 30 μs, and decayed with one exponential, 0.062 ms. The range of peak P_os were produced with peak glutamate concentrations from 2.8 to 3.7 mM, though the changes in peak P_o also could be obtained by altering the time constant of decay by ~30%.

Simulating the EPSC evoked in 2.5 Ca^{2+} was more difficult. Regardless of the glutamate transient, the simulated EPSC decayed faster than the experimental EPSC. This is a result of the rates into the desensitized states necessary to fit the patch data. The discrepancy between the time courses of the simulation and the somatically recorded EPSC could be the result of (1) voltage clamp errors or dendritic filtering, (2) greater release asynchrony at 2.5 Ca^{2+} than at lower concentrations, (3) different kinetics of AMPA receptors in patches than those at synapses, or (4) diffusion of glutamate to more distant receptors when multiple vesicles are released. These issues are addressed in the Discussion section. In the model, however, the amount of inhibition of the peak amplitude of the EPSC by γ-DGG did not depend greatly on late components of the glutamate concentration transient. Therefore, we set the peak P_o at 0.66, as determined from the nonstationary noise analysis of patch currents, assuming near saturation of synaptic AMPA receptors at 2.5 Ca^{2+}. We also assumed that multiple vesicles released at a single synapse were released independently. Thus, because the distribution of their release times should be similar to that across synapses, we convolved the glutamate transient found to mimic the aEPSC with the release time course in Figure 7C to estimate the rise time of the MVR transient (53 μs). With these constraints, in addition to the 17% and 27% inhibition with 1 and 2 mM γ-DGG, we found that a range of glutamate transients can account for the experimental data, two examples of which are given here. The simulated glutamate transient with the lowest peak concentration able to reproduce the data reached 9.2 mM and decayed with one exponential component of 2.2 ms. Lower peak concentrations (8 mM) were also able to mimic the block by γ-DGG; however, the decay of the glutamate transient had to be lengthened to such a degree ($\tau_{decay} > 5$ ms) that the simulated EPSC gained a small but very long tail that was never observed in the experimental EPSCs. In the second example, the glutamate transient peaked at 11.3 mM and decayed with two exponential components of 0.49 ms (96% amplitude) and 4 ms (Figure 8B). Assuming that these peak concentrations (9.2–11.3 mM) result from the near simultaneous release of multiple vesicles into the cleft, each of which would contribute 2.8 to 3.7 mM (see above), the simplest interpretation is that 2.5–4 vesicles are released, on average, per synapse per action potential. The exact number of vesicles released is less important that the qualitative result: The great difference in inhibition of the EPSC at low and high P_r by γ-DGG (e.g., 82% versus 27% at 2 mM) requires very large differences in the glutamate transient.

Discussion

Using a technique devised to estimate the concentration transient of transmitter at postsynaptic receptors, we have shown that the glutamate transient depends on the P_r at the CF-PC synapse: the higher the release probability, the larger the glutamate transient. As spillover and mixing of glutamate released from neighboring synapses cannot account for the elevation in the glutamate transient, we suggest that multiple vesicles can be released at individual synapses following a presynaptic action potential. Kinetic modeling of the AMPA recep-

tors further suggests that the glutamate concentration transient at CF-PC synapses can reach very high concentrations, in the range of 9–12 mM.

The prolonged time course of the EPSC at CF-PC synapses has been a subject of much investigation. Llano et al. (1991) argued that the slow decay time of the EPSC did not result from dendritic filtering or inadequate voltage clamp. Using a voltage jump protocol (Pearce, 1993), Barbour et al. (1994) found that the underlying synaptic current faithfully followed the time course of the underlying synaptic conductance. We used the voltage jump protocol and analysis procedures of Hausser and Roth (1997) and also found that the time course of decay of the synaptic conductance is mimicked by the EPSC recorded at the soma. The slow decay of the CF-PC EPSC, therefore, is not determined by receptor deactivation kinetics as it appears to be at other synapses (Magleby and Stevens, 1972; Lester et al., 1990; Hestrin, 1993; Livsey et al., 1993). Indeed, AMPA receptor kinetics in outside-out patches are much faster than the EPSC (see above; Barbour et al., 1994; Hausser and Roth, 1997), indicating that either AMPA receptor kinetics are different in outside-out patches or that some other mechanism is prolonging the synaptic conductance. Silver et al. (1998) reported that the EPSC decay is longer in normal release conditions than at lower release probabilities and suggested that this could reflect spillover and pooling or that "changes in the release process itself" could give "different transmitter concentration profiles at different release probabilities." The simplest conclusion from these studies is that at the normally high P_r of this synapse (Silver et al., 1998), glutamate is cleared from the synaptic cleft quite slowly.

We have readdressed these questions because glutamate uptake is enhanced at the higher temperatures used in this study and may prevent the spillover and pooling that can occur at room temperature (Asztely et al., 1997). We find that, although the kinetics of both patch and synaptic currents are faster at higher temperatures, AMPA receptor responses in patches are faster than EPSCs, and EPSCs recorded at low P_r are faster than those at high P_r. At least two mechanisms could contribute to a prolonged decay time at high P_r: greater release asynchrony and slower clearance. Release asynchrony probably does not contribute significantly to the time course of the high P_r EPSC, because the time course of release (Figure 7C) at low P_r is brief and release asynchrony is thought to be unaffected by changes in P_r (Barrett and Stevens, 1972; Datyner and Gage, 1980, van der Kloot, 1988; Isaacson and Walmsley, 1995; Diamond and Jahr, 1995). In addition, if the tail of the high P_r EPSC was the result of asynchronous release (i.e., the summation of many single exocytotic events), it would not be entirely blocked by γ-DGG. Rather, it would be blocked to the same degree as the low P_r EPSC, ~80%. Because the tail is completely blocked by γ-DGG, we suggest that the receptors mediating the tail are activated by much lower concentrations of glutamate than achieved by rapid exocytosis. Thus, at high P_r, glutamate clearance is slower than at low P_r, probably because more glutamate is released at high P_r.

We suggest the peak of the EPSC is mediated by glutamate released locally, at individual release sites, because blocking glutamate transport had no affect on the block of the peak EPSC amplitude by γ-DGG. However, during the decay of the EPSC, glutamate certainly spills out of the cleft because it activates both AMPA receptors and glutamate transporters expressed by neighboring Bergmann glial cell membranes (Bergles et al., 1997), where it achieves a concentration near 200 μM (Dzubay and Jahr, 1999). Activation of extrasynaptic AMPA receptors on Purkinje cells may then contribute to the slow decay phase of the high P_r EPSC. In support of this, we find that the high P_r EPSC decays more slowly than the desensitization rate in patches. If we assume (1) that synaptic receptors desensitize at the same rate as those in patches, (2) that all release sites at this high P_r synapse release multiple vesicles, and (3) that this leads to postsynaptic AMPA receptor saturation, then postsynaptic receptors will not be able to support the prolonged EPSC decay even if spillover and pooling occur. We suggest that at high P_r, glutamate spills out of the synapse, overwhelms local transporters expressed by Purkinje and Bergmann glial cells, and activates nearby extrasynaptic AMPA receptors found on Purkinje cell dendrites (Hausser and Roth, 1997). A comparison of the simulated glutamate transients needed to fit the aEPSC and the EPSC recorded in 2.5 mM Ca^{2+} reveals a dramatic slowing of clearance that would require near saturation of local transporter populations. An important caveat to these suggestions is that although the deactivation rate of AMPA receptors in patches is similar to the decay of aEPSCs, we have not been able to assess desensitization rates of AMPA receptors at synapses. If synaptic AMPA receptors desensitize more slowly than receptors in patches, the prolonged EPSC could result from rebinding of glutamate to synaptic receptors.

It has been reported that variations in synaptic glutamate concentrations can arise from different rates of glutamate efflux from synaptic vesicles (Choi et al., 2000; Renger et al., 2001). These studies suggest that some vesicles release their contents slowly at low P_r or early in development, leading to low concentrations of glutamate in the cleft (≪170 μM) (Choi et al., 2000) that, however, last for many milliseconds. At high P_r, exocytosis becomes more explosive, and glutamate rapidly attains high concentrations at postsynaptic receptors. However, CF-PC EPSCs behave in a manner opposite to these predictions. At low P_r, evoked EPSCs rise as fast as at high P_r but decay with a faster time course. Furthermore, the very low synaptic glutamate transients reported to occur at low P_r in hippocampal synapses (≪170 μM, τ_{decay} = 5 ms) are predicted by our model to be blocked by ≫90% by 2 mM γ-DGG, more than we find at the CF-PC synapse. In addition, such glutamate transients produce EPSCs that rise to peak much more slowly than our data indicate. For these reasons, we believe that at the CF-PC synapse, slow release of glutamate from vesicles cannot account for the differential block by γ-DGG.

Previous studies have estimated that glutamate transporters expressed by Purkinje cells take up a significant fraction of glutamate released at climbing fiber synapses, from greater than 22% (Otis et al., 1997) to between 56% and 230% (Auger and Attwell, 2000). Both estimates were based on the amount of glutamate thought to be contained in single vesicles. If MVR is a

regular occurrence, however, much more glutamate is released into the cleft. This may decrease the percentage taken up by Purkinje cells, as the highest density of Purkinje cell transporter expression occurs just outside of the cleft (~1800 per μm^2) (Dehnes et al., 1998). Once these transporters approach saturation, the predominant sink for glutamate is the higher density of transporters expressed by the surrounding Bergmann glial cell membranes (~5400 per μm^2) (Lehre and Danbolt, 1998). As a rather high concentration of glutamate is attained at Bergmann glial AMPA receptors in conditions similar to the present experiments (~200 μM) (Dzubay and Jahr, 1999), a significant escape of glutamate from climbing fiber synapses seems reasonable.

MVR has been reported at inhibitory synapses onto cerebellar Purkinje cells (Auger and Marty, 2000) and at excitatory synapses in culture (Tong and Jahr, 1994; Prange and Murphy, 1999). Does MVR occur at all synapses? If the CF-PC synapse is representative, other synapses should be capable of releasing more than one vesicle. However, the likelihood of releasing more than one vesicle depends, in the present study, on P_r. P_r across synapses varies widely, even across synapses of the same type. For instance, P_r at Schaffer collateral synapses can range from 0 to nearly 1.0 (Dobrunz and Stevens, 1997; Hanse and Gustafsson, 2001). However, most synapses in the central nervous system are thought to have much lower P_r, on average, than that of the climbing fiber. Thus, the probability of releasing two vesicles per release site per action potential normally would be low. Mechanisms that elevate P_r, such as frequency facilitation, decreased presynaptic inhibition, or presynaptically expressed long-term potentiation may increase the probability of MVR, which will likely increase the occupancy of at least AMPA receptors and maybe NMDA receptors (Mainen et al., 1999; McAllister and Stevens, 2000), as well as increasing spillover to pre- and postsynaptic extrasynaptic receptors.

Experimental Procedures

Tissue Preparation

Parasagittal cerebellar slices were prepared from rats aged 11–17 days after Otis et al. (1997). Animals were decapitated, and the cerebellar vermis was dissected out and glued to the stage of a vibroslicer (Leica Instruments) in ice-cold solution containing (in mM) 119 NaCl, 2.5 KCl, 2.5 $CaCl_2$, 1.3 $MgCl_2$, 1 NaH_2PO_4, 26.2 $NaHCO_2$, and 11 glucose, bubbled with 95% O_2–5% CO_2. Slices of 250–300 μm thickness were consecutively cut and incubated at 37°C for 15–30 min before use in electrophysiological recordings. During recordings, the slices were superfused with the solution described previously with the addition of 100 μM picrotoxin to block $GABA_A$ receptors.

Electrophysiology and Perfusion Technique

Whole-cell recordings were made with infrared differential interference contrast optics at 32°C–35°C using a ×40 water-immersion objective on an upright microscope (Zeiss Axioskop) at depolarized membrane potentials (−10 to −20 mV), unless otherwise stated, to decrease the CF-PC EPSCs to manageable amplitudes. Pipettes with resistances of 0.9 to 1.2 MΩ were used. The series resistance, as measured by the instantaneous current response to a 1–5 mV step with only the pipette capacitance canceled, was always less than 5 MΩ (usually less than 3 MΩ). Series resistance was routinely compensated >80%. Pipette solutions contained (in mM) 35 CsF, 100 CsCl, 10 EGTA, and 10 HEPES (pH 7.2) with CsOH. Synaptic transporter currents were recorded at −70 mV in the presence of 25 μM NBQX with a similar pipette solution, except Kgluconate was substituted for CsCl and CsF. Single climbing fibers were stimulated (10–300 μA, 50–100 μs) with a theta glass pipette filled with bath solution and placed in the granule cell layer. The pipette was repositioned, and the stimulus intensity was adjusted until the current required to elicit an all-or-none response was minimized. This is done to eliminate any significant parallel fiber activation. Synaptic and patch currents were filtered at 2–5 kHz and digitized at 20–50 kHz using acquisition software written in Igor Pro software (J.S. Diamond, WaveMetrics, Lake Oswego, OR). For patch experiments, a four barrel glass flow-pipe mounted on a piezoelectric bimorph (Vernitron, Bedford, OH) was used for agonist applications to outside-out patches as described previously (Tong and Jahr, 1994). Solution exchange times (typically < 150 μs) were measured after each experiment by rupturing the patch and recording junction currents across the open pipette tip. All experiments were performed at 32°C –35°C attained with an in-line heating device (Warner Instruments, Hamden, CT). Reported values are the mean ± SD. Data analysis and simulations were done using Igor Pro, AxoGraph (Axon Instruments, Union City, CA), and SCoP (Simulation Resources, Redlands, CA).

Acknowledgments

This work was supported by NS11095 (J.I.W.), HFSP RG119/2000, and NS40056 (C.E.J). We thank Andrew Delaney, John Harrison, Ko Matsui, Caitlin Smith, and Anastassios Tzingounis for discussions and reading the manuscript.

Received May 21, 2001; revised August 1, 2001.

References

Abdul-Ghani, M.A., Valiante, T.A., and Pennefather, P.S. (1996). Sr^{2+} and quantal events at excitatory synapses between mouse hippocampal neurons in culture. J. Physiol. *495*, 113–125.

Alvarez-Leefmans, F.J., De Santis, A., and Miledi, R. (1979). Effects of some divalent cations on synaptic transmission in frog spinal neurones. J. Physiol. *294*, 387–406.

Asztely, F., Erdemli, G., and Kullmann, D.M. (1997). Extrasynaptic glutamate spillover in the hippocampus: dependence on temperature and the role of active glutamate uptake. Neuron *18*, 281–293.

Auger, C., and Attwell, D. (2000). Fast removal of synaptic glutamate by postsynaptic transporters. Neuron *28*, 547–558.

Auger, C., and Marty, A. (2000). Quantal currents at single-site central synapses. J. Physiol. *526*, 3–11.

Auger, C., Kondo, S., and Marty, A. (1998). Multivesicular release at single functional synaptic sites in cerebellar stellate and basket cells. J. Neurosci. *18*, 4532–4547.

Barbour, B., and Hausser, M. (1997). Intersynaptic diffusion of neurotransmitter. Trends Neurosci. *20*, 377–384.

Barbour, B., Keller, B.U., Llano, I., and Marty, A. (1994). Prolonged presence of glutamate during excitatory synaptic transmission to cerebellar Purkinje cells. Neuron *12*, 1331–1343.

Barrett, E.F., and Stevens, C.F. (1972). The kinetics of transmitter release at the frog neuromuscular junction. J. Physiol. *227*, 691–708.

Bergles, D.E., and Jahr, C.E. (1997). Synaptic activation of glutamate transporters in hippocampal astrocytes. Neuron *19*, 1297–1308.

Bergles, D.E., Dzubay, J.A., and Jahr, C.E. (1997). Glutamate transporter currents in bergmann glial cells follow the time course of extrasynaptic glutamate. Proc. Natl. Acad. Sci. USA *94*, 14821–14825.

Choi, S., Klingauf, J., and Tsien, R.W. (2000). Postfusional regulation of cleft glutamate concentration during LTP at "silent synapses." Nat. Neurosci. *3*, 330–336.

Clark, B.A., and Barbour, B. (1997). Currents evoked in Bergmann glial cells by parallel fibre stimulation in rat cerebellar slices. J. Physiol. *502*, 335–350.

Clements, J.D. (1996). Transmitter timecourse in the synaptic cleft: its role in central synaptic function. Trends Neurosci. *19*, 163–171.

Clements, J.D., Lester, R.A., Tong, G., Jahr, C.E., and Westbrook, G.L. (1992). The time course of glutamate in the synaptic cleft. Science *258*, 1498–1501.

Datyner, N.B., and Gage, P.W. (1980). Phasic secretion of acetylcholine at a mammalian neuromuscular junction. J. Physiol. *303*, 299–314.

Dehnes, Y., Chaudhry, F.A., Ullensvang, K., Lehre, K.P., Storm-Mathisen, J., and Danbolt, N.C. (1998). The glutamate transporter EAAT4 in rat cerebellar Purkinje cells: a glutamate-gated chloride channel concentrated near the synapse in parts of the dendritic membrane facing astroglia. J. Neurosci. *18*, 3606–3619.

del Castillo, J., and Katz, B. (1954). Statistical factors involved in neuromuscular facilitation and depression. J. Physiol. *124*, 574–585.

Diamond, J.S., and Jahr, C.E. (1995). Asynchronous release of synaptic vesicles determines the time course of the AMPA receptor-mediated EPSC. Neuron *15*, 1097–1107.

Diamond, J.S., and Jahr, C.E. (1997). Transporters buffer synaptically released glutamate on a submillisecond time scale. J. Neurosci. *17*, 4672–4687.

Dittman, J.S., and Regehr, W.G. (1998). Calcium dependence and recovery kinetics of presynaptic depression at the climbing fiber to Purkinje cell synapse. J. Neurosci. *18*, 6147–6162.

Dobrunz, L.E., and Stevens, C.F. (1997). Heterogeneity of release probability, facilitation, and depletion at central synapses. Neuron *18*, 995–1008.

Dzubay, J.A., and Jahr, C.E. (1999). The concentration of synaptically released glutamate outside of the climbing fiber-Purkinje cell synaptic cleft. J. Neurosci. *19*, 5265–5274.

Eliasof, S., and Jahr, C.E. (1996). The retinal glial cell glutamate transporter is coupled to an anionic conductance. Proc. Natl. Acad. Sci. USA *93*, 4153–4158.

Goda, Y., and Stevens, C.F. (1994). Two components of transmitter release at a central synapse. Proc. Natl. Acad. Sci. USA *91*, 12942–12946.

Hanse, E., and Gustafsson, B. (2001). Vesicle release probability and pre-primed pool at glutamatergic synapses in area CA1 of the rat neonatal hippocampus. J. Physiol. *531*, 481–493.

Hashimoto, K., and Kano, M. (1998). Presynaptic origin of paired-pulse depression at climbing fibre-Purkinje cell synapses in the rat cerebellum. J. Physiol. *506*, 391–405.

Hausser, M., and Roth, A. (1997). Dendritic and somatic glutamate receptor channels in rat cerebellar Purkinje cells. J. Physiol. *501*, 77–95.

Hestrin, S. (1993). Different glutamate receptor channels mediate fast excitatory synaptic currents in inhibitory and excitatory cortical neurons. Neuron *11*, 1083–1091.

Heuser, J.E., Reese, T.S., Dennis, M.J., Jan, Y., Jan, L., and Evans, L. (1979). Synaptic vesicle exocytosis captured by quick freezing and correlated with quantal transmitter release. J. Cell Biol. *81*, 275–300.

Isaacson, J.S., and Walmsley, B. (1995). Counting quanta: direct measurements of transmitter release at a central synapse. Neuron *15*, 875–884.

Konnerth, A., Llano, I., and Armstrong, C.M. (1990). Synaptic currents in cerebellar Purkinje cells. Proc. Natl. Acad. Sci. USA *87*, 2662–2665.

Korn, H., Sur, C., Charpier, S., Legendre, P., and Faber, D.S. (1994). The one-vesicle hypothesis and multivesicular release. In Molecular and Cellular Mechanisms of Neurotransmitter Release, L. Stjarne, P. Greengard, S. Grillner, T. Hokfelt, and D. Ottoson, eds. (New York: Raven Press), pp. 301–322.

Llano, I., Marty, A., Armstrong, C.M., and Konnerth, A. (1991). Synaptic- and agonist-induced excitatory currents of Purkinje cells in rat cerebellar slices. J. Physiol. *434*, 183–213.

Lehre, K.P., and Danbolt, N.C. (1998). The number of glutamate transporter subtype molecules at glutamatergic synapses: chemical and stereological quantification in young adult rat brain. J. Neurosci. *18*, 8751–8757.

Lester, R.A.J., Clements, J.D., Westbrook, G.L., and Jahr, C.E. (1990). Channel kinetics determine the time course of NMDA-receptor mediated synaptic currents. Nature *346*, 565–567.

Liu, G., Choi, S., and Tsien, R.W. (1999). Variability of neurotransmitter concentration and nonsaturation of postsynaptic AMPA receptors at synapses in hippocampal cultures and slices. Neuron *22*, 395–409.

Livsey, C.T., Costa, E., and Vicini, S. (1993). Glutamate-activated currents in outside-out patches from spiny versus aspiny hilar neurons of rat hippocampal slices. J. Neurosci. *13*, 5324–5333.

Magleby, K.L., and Stevens, C.F. (1972). The effect of voltage on the time course of end-plate currents. J. Physiol. *223*, 151–171.

Mainen, Z.F., Malinow, R., and Svoboda, K. (1999). Synaptic calcium transients in single spines indicate that NMDA receptors are not saturated. Nature *399*, 151–155.

McAllister A.K., and Stevens, C.F. (2000). Nonsaturation of AMPA and NMDA receptors at hippocampal synapses. Proc. Natl. Acad. Sci. USA *97*, 6173–6178.

Otis, T.S., Wu, Y.C., and Trussell, L.O. (1996). Delayed clearance of transmitter and the role of glutamate transporters at synapses with multiple release sites. J. Neurosci. *16*, 1634–1644.

Otis, T.S., Kavanaugh, M.P., and Jahr, C.E. (1997). Postsynaptic glutamate transport at the climbing fiber-Purkinje cell synapse. Science *277*, 1515–1518.

Palay, S.L., and Chan-Palay, V. (1974). Cerebellar Cortex: Cytology and Organization (New York: Springer-Verlag).

Pearce, R.A. (1993). Physiological evidence for two distinct GABAA responses in rat hippocampus. Neuron *10*, 189–200.

Prange, O., and Murphy, T.H. (1999). Analysis of multiquantal transmitter release from single cultured cortical neuron terminals. J. Neurophysiol. *81*, 1810–1817.

Redman, S. (1990). Quantal analysis of synaptic potentials in neurons of the central nervous system. Physiol. Rev. *70*, 165–198.

Renger, J.J., Egles, C., and Liu, G. (2001). A developmental switch in neurotransmitter flux enhances synaptic efficacy by affecting AMPA receptor activation. Neuron *29*, 469–484.

Rusakov, D.A., and Kullmann, D.M. (1998). A tortuous and viscous route to understanding diffusion in the brain. Trends Neurosci. *21*, 469–470.

Schikorski, T., and Stevens, C.F. (2001). Morphological correlates of functionally defined synaptic vesicle populations. Nat. Neurosci. *4*, 391–395.

Shimamoto, K., Lebrun, B., Yasuda-Kamatani, Y., Sakaitani, M., Shigeri, Y., Yumoto, N., and Nakajima, T. (1998). DL-threo-beta-benzyloxyaspartate, a potent blocker of excitatory amino acid transporters. Mol. Pharmacol. *53*, 195–201.

Sigworth, F.J. (1980). The variance of sodium current fluctuations at the node of Ranvier. J. Physiol. *307*, 97–129.

Silver, R.A., Momiyama, A., and Cull-Candy, S.G. (1998). Locus of frequency-dependent depression identified with multiple-probability fluctuation analysis at rat climbing fibre-Purkinje cell synapses. J. Physiol. *510*, 881–902.

Sorra, K.E., and Harris, K.M. (1993). Occurrence and three-dimensional structure of multiple synapses between individual radiatum axons and their target pyramidal cells in hippocampal area CA1. J. Neurosci. *13*, 3736–3748.

Spacek, J. (1985). Three-dimensional analysis of dendritic spines. II. Spine apparatus and other cytoplasmic components. Anat. Embryol. *171*, 235–243.

Tong, G., and Jahr, C.E. (1994). Multivesicular release from excitatory synapses of cultured hippocampal neurons. Neuron *12*, 51–59.

Van der Kloot, W. (1988). Estimating the timing of quantal releases during end-plate currents at the frog neuromuscular junction. J. Physiol. *402*, 595–603.

Ventura, R., and Harris, K.M. (1999). Three-dimensional relationships between hippocampal synapses and astrocytes. J. Neurosci. *19*, 6897–6906.

Wadiche, J.I., and Kavanaugh, M.P. (1998). Macroscopic and micro-

scopic properties of a cloned glutamate transporter/chloride channel. J. Neurosci. *18*, 7650–7661.

Wadiche, J.I., Amara, S.G., and Kavanaugh, M.P. (1995). Ion fluxes associated with excitatory amino acid transport. Neuron *15*, 721–728.

Watkins, J.C. (1991). Some chemical highlights in the development of excitatory amino acid pharmacology. Can. J. Physiol. Pharmacol. *69*, 1064–1075.

Xu-Friedman, M.A., Harris, K.M., and Regehr, W.G. (2001). Three-dimensional comparison of ultrastructural characteristics at depressing and facilitating synapses onto cerebellar Purkinje cells. J. Neurosci. *21*, 6666–6672.

Zerangue, N., and Kavanaugh, M.P. (1996). Flux coupling in a neuronal glutamate transporter. Nature *383*, 634–637.